

Band Structure and Quantum Conductance of Nanostructures from Maximally-Localized Wannier Functions: The Case of Functionalized Carbon Nanotubes

Young-Su Lee,¹ Marco Buongiorno Nardelli,² and Nicola Marzari¹

¹*Department of Materials Science and Engineering and Institute for Soldier Nanotechnologies,
Massachusetts Institute of Technology, Cambridge, MA 02139, USA*

²*Center for High Performance Simulations (CHiPS) and Department of Physics,
North Carolina State University, Raleigh, NC 27695, USA
and CCS-CSM, Oak Ridge National Laboratory, Oak Ridge, TN 37831, USA*

(Dated: September 7, 2018)

We have combined large-scale, Γ -point electronic-structure calculations with the maximally-localized Wannier functions approach to calculate efficiently the band structure and the quantum conductance of complex systems containing thousands of atoms while maintaining full first-principles accuracy. We have applied this approach to study covalent functionalizations in metallic single-walled carbon nanotubes. We find that the band structure around the Fermi energy is much less dependent on the chemical nature of the ligands than on the sp^3 functionalization pattern disrupting the conjugation network. Common aryl functionalizations are more stable when paired with saturating hydrogens; even when paired, they still act as strong scattering centers that degrade the ballistic conductance of the nanotubes already at low degrees of coverage.

Carbon nanotubes (CNTs) are some of the most promising materials in micro- and nano-electronics, whose applications could range from transistors to interconnects to memories [1]. In the present effort to engineer and tune the electronic properties of CNTs, organic functionalizations of the sidewalls provide one of the most encouraging avenues [2, 3], ideally combining the exceptional electronic properties of CNTs with the diversity of organic chemistry. In this Letter, we study the effects of covalent functionalizations on single-walled CNTs using a novel approach to calculate the electronic structure and quantum conductance, based on our idea of constructing well-localized and transferable orbitals as ideal building blocks for the electronic structure of complex nanostructures [4, 5, 6, 7]. These maximally-localized Wannier functions (MLWFs) provide a most compact and most accurate local representation of the electronic structure of a solid or a molecule, and are used to construct the full Hamiltonian and to derive the band structure and the Landauer conductance of complex systems containing at least thousands of atoms, preserving first-principles accuracy and with linear-scaling computational costs.

Pristine, single-walled CNTs are ideal one-dimensional quantum wires with quasi-ballistic electron transport for tens of nanometers (at low bias) even at room temperature [8, 9]. Structural or electronic defects and inelastic excitations are then some of the most relevant factors which limit conductance. Covalent functionalizations will alter conduction manifolds and doping levels, thus affecting significantly the electronic transport properties of CNTs [10]. First-principles approaches are especially suited to characterize such effects, in the controlled environment of quantum-mechanical simulations. Here, we use density-functional theory in the GGA-PBE approximation [11], using state-of-the-art solid-state approaches

[12]. Explicit first-principles calculations of systems containing thousands of atoms are rarely possible [13], and the delocalized nature of the Bloch orbitals is not well-suited to describe the transport properties of aperiodic systems; these obstacles are overcome by the approach described in the following.

Disentanglement and Localization: Our method starts from the construction of an optimal MLWFs basis set. In a large supercell, where the sampling of the Brillouin zone (BZ) is limited to the Γ -point, MLWFs can be obtained by a unitary transformation of the occupied ground-state eigenfunctions $\{|\psi_m\rangle\}$: $|w_n\rangle = \sum_{m=1}^{N_{occ}} U_{mn} |\psi_m\rangle$, where U is chosen to minimize the sum of the spread of all $|w_n\rangle$ around their centers [4, 14]. This is not a viable approach for metallic systems, or even for insulators where the occupied subspace can significantly change character as we move away from Γ , even if for the supercell at hand Γ -sampling might be adequate to calculate the energy and charge density of the system with the necessary accuracy. Our goal is instead to obtain, from a combination of the occupied and some of the unoccupied eigenfunctions at Γ , a compact and localized set of orbitals that describes a group of bands of interest (i.e., manifold) in the whole BZ of the supercell - similar in spirit to the $\mathbf{k} \cdot \mathbf{p}$ method [15], but with a different approach and improved outcome. This optimal set is obtained with a two-step procedure. First, an optimally-smooth subspace is extracted from the Hilbert space (i.e., “disentangled”), using a procedure recently introduced [5] and specifically adapted here to the case of Γ -sampling. This N -dimensional subspace consists of a linear combination of all N_o eigenstates at Γ that fall inside a given energy window (with $N_o > N$), and is chosen so that its dispersion across the BZ is as small as possible: this is akin to say that its projection operator

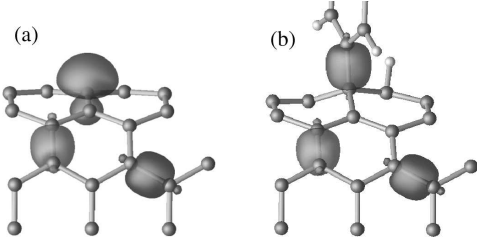


FIG. 1: MLWFs obtained from the disentanglement and localization procedure. We show in (a) the 3 inequivalent MLWFs obtained for a pristine metallic (5,5) CNT, clearly corresponding to a chemical picture of p_z and sp^2 orbitals, and in (b) the same MLWFs for the case when an aminophenyl group (1% coverage) has been covalently attached.

has a minimal change of character as the BZ is swept, or that the basis set obtained is as complete as possible. This subspace is identified by its projection operator $\hat{P}(\Gamma) = \sum_{n=1}^N |\phi_n\rangle\langle\phi_n|$, where $|\phi_n\rangle = \sum_{m=1}^{N_o} A_{mn} |\psi_m\rangle$. The $N_o \times N$ matrix A (such as $A^\dagger A = \mathbf{I}$) is the key quantity to be determined, and is chosen so that the projection operator at Γ has maximal overlap with its first neighbors, i.e., it maximizes $\sum_l W_l \text{Tr}[\hat{P}(\Gamma) \hat{P}(\mathbf{G}_l)]$, where the neighbors \mathbf{G}_l and the weight factors W_l are chosen according to Refs. [4, 14]. Once this optimally-smooth manifold is extracted, a standard localization procedure can be applied on the $\{|\phi_n\rangle\}$ to obtain MLWFs $\{|w_n\rangle\}$. *Band Structure and Quantum Conductance:* The procedure outlined above corresponds to an inverse mapping of first-principles, extended Bloch orbitals into tight-binding orbitals $|w_{n\mathbf{R}}\rangle = |w_n(\mathbf{r} - \mathbf{R})\rangle$ that are then periodically repeated to generate, via Bloch sums, wavefunctions at any arbitrary \mathbf{k} : $|\psi_{n\mathbf{k}}\rangle = \frac{1}{\sqrt{N_R}} \sum_{\mathbf{R}} e^{i\mathbf{k}\cdot\mathbf{R}} |w_{n\mathbf{R}}\rangle$ (\mathbf{R} and \mathbf{k} refer to the direct and reciprocal spaces of the supercell). Localization allows us to neglect in the resulting Hamiltonian matrix all terms $\langle w_{m\mathbf{R}} | \hat{H} | w_{n\mathbf{R}'} \rangle$ for which $|\mathbf{r}_{m\mathbf{R}} - \mathbf{r}_{n\mathbf{R}'}| > L$, with $\mathbf{r}_{m\mathbf{R}}$ the center of $|w_{m\mathbf{R}}\rangle$, and L a cutoff distance determined by the spread of the MLWFs. Since these MLWFs span both the occupied and unoccupied subspaces, they will be well-localized and decay exponentially [16] even in metals. The Hamiltonian matrix becomes diagonally-dominant, and is straightforwardly given by

$$\langle \psi_{m\mathbf{k}} | \hat{H} | \psi_{n\mathbf{k}} \rangle = \langle w_{m0} | \hat{H} | w_{n0} \rangle + \sum_{\mathbf{R}} e^{i\mathbf{k}\cdot\mathbf{R}} \langle w_{m0} | \hat{H} | w_{n\mathbf{R}} \rangle \quad (1)$$

where the sum runs only over the very few supercells (two, for 1-dimensional nanotubes) interacting with the one at the origin. The advanced and retarded Green functions $G_C^{a,r}$ of the conductor and the couplings with the left or right lead $\Gamma_{L,R}$ can be derived from the matrix elements of the Hamiltonian, providing the equilibrium Landauer conductance $\mathcal{G}(E) = \frac{2e^2}{h} \text{Tr}(\Gamma_L G_C^r \Gamma_R G_C^a)$ (see Refs. [6, 17, 18, 19] for detailed explanations of this approach and its implementation in periodic bound-

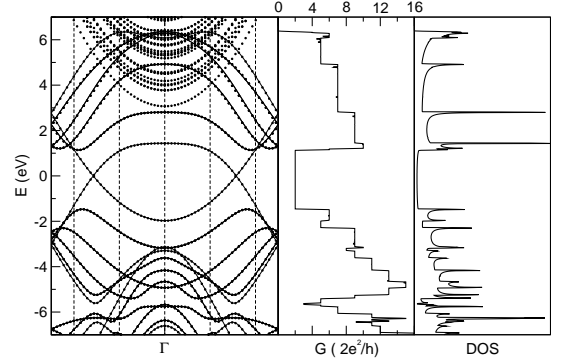


FIG. 2: Band structure, quantum conductance, and density of states of a (5,5) CNT as calculated in the present approach based on MLWFs (solid lines), and compared with the results of a full diagonalization (circles). The band structure has been unfolded over the BZ corresponding to the primitive 20-atom unit cell; the five vertical dashed lines indicate the 5 \mathbf{k} -points corresponding to Γ in a 100-atom supercell.

ary conditions). As a validation, we first calculate the band structure and the quantum conductance of a pristine (5,5) CNT in a 100-atom supercell. The manifold of interest is that spanned by the bonding combination of sp^2 orbitals (the graphitic backbone) and by the p_z orbitals (π and π^* bands), so the disentanglement and localization procedure uses a target dimension of 2.5 orbitals per atom. We show in Fig. 1 the resulting MLWFs, confirming this intuitive chemical picture. In addition, the right panel shows the case of an aminophenyl functionalization, where the “half-filled” p_z orbital is replaced by an sp^3 bonding orbital. The two other MLWFs barely show any change, clearly hinting at the fact that maximal-localization corresponds also to maximal-transferability of the MLWFs building blocks. Once the (short-ranged) matrix elements of the Hamiltonian have been determined, the band structure at any point in the BZ can be obtained with negligible computational costs by diagonalization of Eq. (1). Results are shown in Fig. 2, and compared with the band structure obtained from a diagonalization in a complete plane-wave basis. The agreement between the two calculations is excellent - essentially a proof of the proper disentanglement of the two manifolds (represented by solid lines and circles) and localization of the MLWFs. The extrema in the band structure and the steps and peaks in the quantum conductance and the density of states are also all in perfect agreement. Even more significantly, the massless bands, the quantum conductance, and the density of states around the Fermi energy clearly display the metallic character of the nanotube, *notwithstanding the fact that the MLWFs have been obtained from the eigenstates at Γ in the presence of a pseudo-gap of ~ 2 eV in the folded BZ*. The reason for this agreement is that, moving away from Γ , the change in character of the occupied manifold is described exactly, for all practical purposes, by the unoccupied part at Γ of

our extracted manifold.

These tools now allow us to study with full first-principles accuracy very complex structures, where the MLWFs obtained from a calculation at Γ or even from an isolated fragment (e.g., a hydrogenated nanotube fragment) will reproduce accurately the fine details of a much larger extended system. We focus here on metallic CNTs whose sidewalls are functionalized for tens of nanometers with a disperse array of covalent ligands. Functionalization with aryl groups has been recently accomplished [20], and our goal is to characterize the effects of electronegative or electropositive ligands such as nitro- or amino-phenyls on the band structure and transport properties of CNTs. It is important to stress that the addition of a covalent ligand can affect nearby sidewall carbons, and expedite further reactions that reduce the local strain energy or minimize the disruption of the conjugated manifold, as observed in fullerenes [21]. While exhaustive studies are necessary to fully characterize the thermodynamic stability of the functional group decorations [22, 23, 24] or the subtle spin polarization they might induce [25], we found that, once a functional group (FG₁) is covalently bound to the sidewall, the attachment of a second one (FG₂) to a nearby carbon becomes more facile. These reactions are strongly site-dependent; we present in Fig. 3 the first and second attachment energies, ΔE_1 and ΔE_2 , corresponding to $\text{CNT} + (\text{FG}_1)\text{H} \rightarrow \text{CNT}(\text{FG}_1) + 1/2\text{H}_2$ and $\text{CNT}(\text{FG}_1) + (\text{FG}_2)\text{H} \rightarrow \text{CNT}(\text{FG}_1)(\text{FG}_2) + 1/2\text{H}_2$ respectively [26]. In order to understand how the electronic structure of the tube is modified by the presence of the ligands, we first studied a periodic array of functionalized pairs in the configuration (α) of Fig. 3, at a density of 1 pair per 100 carbons. The resulting band structures are shown in Fig. 4, for the cases where the functional group pairs are composed either by two hydrogen atoms, or a nitro- or aminophenyl and a hydrogen. For comparison, we also report the band structure of the pristine CNT (folded in the BZ of the supercell), and the one obtained

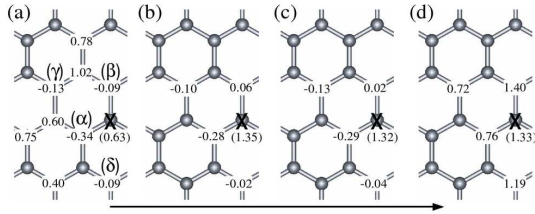


FIG. 3: ΔE_2 in eV as a function of the position of the functional group FG₂ when the group FG₁ is attached in the position marked by X (ΔE_1 is indicated in parenthesis) on a (5,5) CNT. FG₁ and FG₂ are, respectively, (a) H and H, (b) nitrophenyl and H, (c) aminophenyl and H, (d) phenyl and phenyl (in our calculation, the nitro and amino residues are in the para position). The arrow lies parallel to the nanotube axis, and we denoted with α , β , γ , and δ the arrangements for four of the most stable pairings.

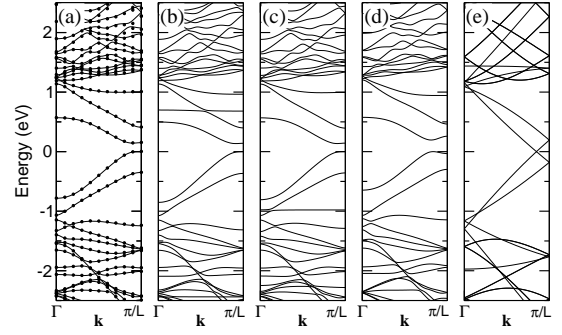


FIG. 4: Band structure of a (5,5) CNT decorated with a periodic array of functionalization pairs in position α (1 pair every 100 carbons): (a) H pair (dots are from a Quantum-Espresso calculation [12], for comparison), (b) nitrophenyl and H, (c) aminophenyl and H, (d) model calculation, where the 2 p_z MLWFs on the functionalized sidewall carbons have been removed from the calculation, (e) pristine nanotube.

from the pristine CNT but removing the two p_z MLWFs sitting on the two sidewall carbon atoms at (α). Interestingly, these band structures are largely insensitive to the chemical nature of the attached groups, notwithstanding the charge transfer taking place when e.g., aminophenyl is substituted for nitrophenyl (0.1 $|e|$ per 100 atoms), or the chemical differences between a phenyl moiety and a hydrogen. The foremost effects on the bands around the Fermi energy are described by a simple model in which the functionalized sidewall carbons change hybridization from sp^2 to sp^3 . Functionalization transforms the p_z MLWF into a bonding sp^3 MLWF whose on-site energy, roughly lowered by 7 eV, removes it altogether from the π conduction manifold; this effect is clearly captured by the model (Fig. 4(d)). A perfectly periodic array of functional pairs might be quite unrealistic; from the transport point of view, the fundamental quantity of interest is the reduction in the transmission probability as more and more groups are attached to a functionalized segment of an otherwise pristine nanotube (see the top of Fig. 5). Our approach is particularly suited to study such complex cases. We show first in the left panels of Fig. 5 the Landauer conductance as a function of energy for an infinite (5,5) CNT with either one pair attached in positions (α), (β), (γ), and (δ) or a single covalent functional group. The covalently-bonded groups act as strong scattering centers, reducing the conductance at the Fermi energy by 19%, 8%, 21%, 17% and 42% respectively. Again, the dominant factors are geometric and similar results are obtained, say, from hydrogen attachments (dashed line) or the removal of p_z MLWFs on the relevant sidewall carbons (solid line). Once a random array of functional groups covers the nanotube for tens of nanometers - comparable to the lengths of pristine tubes for which we can observe ballistic transport [8] - the conductance of the tube drops dramatically, as shown in the

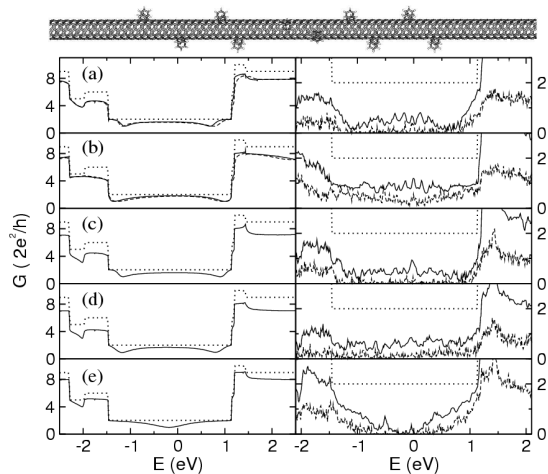


FIG. 5: Top: infinite metallic (5,5) CNT functionalized in its central region by an array of phenyl pairs. Left panel: quantum conductance of an infinite (5,5) CNT with one isolated pair of ligands in positions α (a), β (b), γ (c), δ (d), or with a single ligand attached (e) (dashed line: ligands are hydrogen atoms; solid line: model calculation; dotted line: pristine CNT). Right panel: random distributions of pairs of ligands or of single ligands (arranged as in the left panel), for the case of 10 defects per 1000 carbons (solid line) or 30 per 3000 (dashed line), averaged over 5 random configurations.

right panels of Fig. 5, for the case of a functionalized conductor 12.3 or 37.0 nm long (corresponding to 1000 or 3000 carbons) between semi-infinite leads. We note that substitutional dopants such as boron and nitrogen also introduce substantial (albeit weaker) disorder, and can change the transport regime from ballistic to localized [28]. Among the patterns studied, β turns out to be the weakest scattering center, since it is a paired defect that preserves the mirror plane containing the tube axis and is almost transparent to either of the two Bloch states with well-defined parity over the mirror plane (a similar result has been discussed for symmetric Stone-Wales defects on a (10,10) CNT [29]).

In conclusion, we have presented a novel approach to calculate the band structure and transport properties of complex nanostructures from large-scale electronic-structure calculations at the Γ point via an essentially exact inverse mapping into explicit and localized tight-binding orbitals (MLWFs). These MLWFs act as electronic-structure building blocks, representing at the same time a minimal and most accurate basis set for the Hilbert space at hand and providing a natural avenue to map first-principles calculations into model Hamiltonians. An application of this approach to covalently-functionalized metallic CNTs provides a clear correlation between chemical bonding and transport properties, showing that the band structure around the Fermi energy is strongly influenced by the sp^3 functionalization pattern disrupting the conjugation network. Common

aryl functionalizations were found to be more stable when clustered with saturating hydrogens; even when paired, they still act as strong scattering centers that degrade the ballistic conductance of carbon nanotubes already at low degrees of functionalization.

The authors would like to thank Y. Wu (Harvard University), P. Giannozzi (Scuola Normale Superiore), and M. Sharma and R. Car (Princeton University) for the collaborative development of an ultrasoft implementation of MLWFs in the Quantum-Espresso package. This research has been supported by MIT Institute for Soldier Nanotechnologies (ISN-ARO DAAD 19-02-D-0002) and the National Science Foundation (NSF-NIRT DMR-0304019). M.B.N. acknowledges funding from the Department of Energy (DE-AC05-00OR22725).

-
- [1] Ph. Avouris, MRS Bull. **29**, 403 (2004).
 - [2] Y.-P. Sun et al., Acc. Chem. Res. **35**, 1096 (2002); D. Tasis et al., Chem. Eur. J. **9**, 4000 (2003).
 - [3] M.S. Strano et al., Science **301**, 1519 (2003); P.-W. Chiu, M. Kaempgen, and S. Roth, Phys. Rev. Lett. **92**, 246802 (2004).
 - [4] N. Marzari and D. Vanderbilt, Phys. Rev. B **56**, 12847 (1997).
 - [5] I. Souza, N. Marzari, and D. Vanderbilt, Phys. Rev. B **65**, 035109 (2002).
 - [6] A. Calzolari et al., Phys. Rev. B **69**, 035108 (2004).
 - [7] K.S. Thygesen and K.W. Jacobsen, Phys. Rev. Lett. **94**, 036807 (2005).
 - [8] A. Javey et al., Phys. Rev. Lett. **92**, 106804 (2004); A. Javey et al., Proc. Natl. Acad. Sci. **101**, 13408 (2004).
 - [9] J.-Y. Park et al., Nano Lett. **4**, 517 (2004).
 - [10] K. Kamaras et al., Science **301**, 1501 (2003).
 - [11] J.P. Perdew, K. Burke, and M. Ernzerhof, Phys. Rev. Lett. **77**, 3865 (1996).
 - [12] S. Baroni et al., <http://www.quantum-espresso.org>.
 - [13] L.-W. Wang, A. Franceschetti, and A. Zunger, Phys. Rev. Lett. **78**, 2819 (1997); L.-W. Wang, Phys. Rev. Lett. **88**, 256402 (2002); C.-K. Skylaris et al., J. Chem. Phys. **122**, 084119 (2005).
 - [14] P.L. Silvestrelli et al., Solid State Commun. **107**, 7 (1998).
 - [15] S. Scandolo and J. Kohanoff, Phys. Rev. B **62**, 15499 (2000).
 - [16] L. He and D. Vanderbilt, Phys. Rev. Lett. **86**, 5341 (2001).
 - [17] S. Datta, *Electronic Transport in Mesoscopic Systems* (Cambridge University Press, Cambridge, 1995).
 - [18] M. Buongiorno Nardelli, Phys. Rev. B **60**, 7828 (1999).
 - [19] J. Taylor, H. Guo, and J. Wang, Phys. Rev. B **63**, 245407 (2001).
 - [20] J.L. Bahr et al., J. Am. Chem. Soc. **123**, 6536 (2001); C.A. Dyke and J.M. Tour, Nano Lett. **3**, 1215 (2003).
 - [21] F. Diederich and C. Thilgen, Science **271**, 317 (1993); C.C. Henderson and P.A. Cahill, Science **259**, 1885 (1993); S. Niyogi et al., Acc. Chem. Res. **35**, 1105 (2002).
 - [22] D. Stojkovic et al., Phys. Rev. B **68**, 195406 (2003).
 - [23] K.F. Kelly et al., Chem. Phys. Lett. **313**, 445 (1999).

- [24] K.A. Worsley, K.R. Moonosawmy, and P. Kruse, Nano Lett. **4**, 1541 (2004).
- [25] E.J. Duplock, M. Scheffler, and P.J.D. Lindan, Phys. Rev. Lett. **92**, 225502 (2004).
- [26] These energies are calculated using 5 \mathbf{k} -points in the 100-atom supercell, spin-polarized GGA-PBE, and 0.02 Ry of cold smearing [27].
- [27] N. Marzari et al., Phys. Rev. Lett. **82**, 3296 (1999).
- [28] S. Latil et al., Phys. Rev. Lett. **92**, 256805 (2004).
- [29] H.J. Choi and J. Ihm, Phys. Rev. B **59**, 2267 (1999).